Controlled Dual Growth Factor Delivery From Microparticles Incorporated Within Human Bone Marrow-Derived Mesenchymal Stem Cell Aggregates for Enhanced Bone Tissue Engineering via Endochondral Ossification

PHUONG N. DANG,[a] NEHA DWIVEDI,[a] LAUREN M. PHILLIPS,[a] XIAOHUA YU,[b] SAMUEL HERBERG,[a] CAITLIN BOWERMAN,[a] LORAN D. SOLORIO,[a] WILLIAM L. MURPHY,[b,c] EBEN ALSBERG[a,d]

Key Words. Bone • Tissue regeneration • High-density culture • Adult human bone marrow • Mesenchymal stem cells • Growth factor delivery

Departments of [a]Biomedical Engineering and [d]Orthopaedic Surgery, Case Western Reserve University, Cleveland, Ohio, USA; Departments of [b]Biomedical Engineering and [c]Orthopedics and Rehabilitation, University of Wisconsin, Madison, Wisconsin, USA

Correspondence: Eben Alsberg, Ph.D., Department of Biomedical Engineering, Case Western Reserve University, 10900 Euclid Avenue, Cleveland, Ohio 44106, USA. Telephone: 216-368-6425; E-Mail: eben.alsberg@case.edu

ABSTRACT

Bone tissue engineering via endochondral ossification has been explored by chondrogenically priming cells using soluble mediators for at least 3 weeks to produce a hypertrophic cartilage template. Although recapitulation of endochondral ossification has been achieved, long-term in vitro culture is required for priming cells through repeated supplementation of inductive factors in the media. To address this challenge, a microparticle-based growth factor delivery system was engineered to drive endochondral ossification within human bone marrow-derived mesenchymal stem cell (hMSC) aggregates. Sequential exogenous presentation of soluble transforming growth factor-β1 (TGF-β1) and bone morphogenetic protein-2 (BMP-2) at various defined time courses resulted in varying degrees of chondrogenesis and osteogenesis as demonstrated by glycosaminoglycan and calcium content. The time course that best induced endochondral ossification was used to guide the development of the microparticle-based controlled delivery system for TGF-β1 and BMP-2. Gelatin microparticles capable of relatively rapid release of TGF-β1 and mineral-coated hydroxyapatite microparticles permitting more sustained release of BMP-2 were then incorporated within hMSC aggregates and cultured for 5 weeks following the predetermined time course for sequential presentation of bioactive signals. Compared with cell-only aggregates treated with exogenous growth factors, aggregates with incorporated TGF-β1- and BMP-2-loaded microparticles exhibited enhanced chondrogenesis and alkaline phosphatase activity at week 2 and a greater degree of mineralization by week 5. Staining for types I and II collagen, osteopontin, and osteocalcin revealed the presence of cartilage and bone. This microparticle-incorporated system has potential as a readily implantable therapy for healing bone defects without the need for long-term in vitro chondrogenic priming. STEM CELLS TRANSLATIONAL MEDICINE 2016;5:206–217

SIGNIFICANCE

This study demonstrates the regulation of chondrogenesis and osteogenesis with regard to endochondral bone formation in high-density stem cell systems through the controlled presentation of inductive factors from incorporated microparticles. This work lays the foundation for a rapidly implantable tissue engineering system that promotes bone repair via endochondral ossification, a pathway that can delay the need for a functional vascular network and has an intrinsic ability to promote angiogenesis. The modular nature of this system lends well to using different cell types and/or growth factors to induce endochondral bone formation, as well as the production of other tissue types.

INTRODUCTION

Current therapies for treating critically sized bone defects are associated with extensive drawbacks, creating a need for alternative approaches [1]. Even autografts, the gold standard, are costly, painful, and restricted in size and shape by limited graft availability [2]. Bone tissue engineering has emerged as a promising alternative to provide regenerative treatment potentially without the limitations of current therapies. The intramembranous ossification pathway has been extensively explored in bone tissue engineering [3], but it is limited by the lack of a functional vascular network to provide nutrients and oxygen for cells during the initial stages of repair [4, 5]. For

example, porous scaffolds seeded with rat bone marrow stromal cells implanted in vivo formed a layer of mineralized tissue only 200–400 μm thick, whereas cells in the interior region did not survive, likely because of nutrient diffusion limitations [4]. Strategies to form bone via a cartilaginous intermediate or endochondral ossification may circumvent issues with supplying nutrients and oxygen early on. Cartilage is an avascular tissue, and chondrocytes have lower metabolic needs, permitting them to survive in microenvironmental conditions with limited nutrients and oxygen [6, 7]. Moreover, endochondral ossification has an internal mechanism for stimulating angiogenesis. It yields hypertrophic chondrocytes that express angiogenic factors such as vascular endothelial growth factor (VEGF), an essential coordinator of angiogenesis, bone development, and fracture repair [8–10]. Thus, this approach has the ability to promote vascular invasion of the construct once in vivo, in addition to delaying the need for an initial vascular supply.

The endochondral ossification pathway has been investigated in high-density cell cultures (e.g., aggregates [11–14] and cell sheets [15]) of human bone marrow-derived mesenchymal stem cells (hMSCs), easily accessible multipotent cells that can maintain their differentiation capacity after expansion [16]. These systems provide a three-dimensional environment with abundant cell-cell interactions that mimic MSC condensation during embryonic development [17, 18]. In a study to promote endochondral ossification, Muraglia et al. [14] observed a hypertrophic cartilage core surrounded by a mineralized shell in hMSC aggregates cultured in chondrogenic medium containing transforming growth factor-β1 (TGF-β1) for 4 weeks followed by 1–3 weeks in osteogenic medium containing dexamethasone, ascorbic acid, and β-glycerophosphate. Additionally, hMSC sheets cultured in vitro in chondrogenic medium for 3 weeks followed by 2 weeks in hypertrophic medium containing β-glycerophosphate and L-thyroxin, a thyroid hormone capable of inducing chondrocyte hypertrophy, formed trabecular bone-like tissue 8 weeks after subcutaneous implantation in mice [15]. Although successful in recapitulating endochondral ossification, these approaches require supplementation of growth factors in media to deliver signals to cells comprising the constructs. This mode of delivery requires extensive in vitro culture because repeated supplementation is necessary to promote cell differentiation. Moreover, as they diffuse to the construct interior, soluble factors may bind to newly formed extracellular matrix or get taken up by cells along their path, decreasing the concentration reaching cells in the interior. The limited spatial control of delivery may lead to slower and/or nonuniform tissue formation that could compromise the integrity of the engineered construct.

Our laboratory has attempted to address these challenges for cartilage tissue engineering based on high-density cell constructs by demonstrating the capacity to drive chondrogenesis via incorporation of growth factor-laden microparticles within these three-dimensional cultures [19–22]. It was demonstrated that neocartilage formation in hMSC aggregates [20] and self-assembled sheets [19] was enhanced with TGF-β1-loaded low-cross-linked gelatin microparticles distributed throughout the constructs. Sheets incorporated with low-cross-linked microparticles had higher glycosaminoglycan (GAG) content and stained more intensely for GAG and type II collagen compared with cell-only constructs treated with exogenously supplemented TGF-β1 [19]. Additionally, microparticle-incorporated sheets were thicker and more mechanically robust than cell-only sheets.

In these dynamic systems, microparticle and growth factor concentrations, as well as the microparticle degradation rate, which is regulated by biopolymer cross-linking density, can be varied to manipulate growth factor distribution and temporal presentation to control chondrogenesis.

The ability to enhance chondrogenesis within high-density hMSC systems by locally delivering TGF-β1 in a controlled manner inspired the application of this approach to delivering inductive signals for bone tissue engineering. A system of hMSC aggregates incorporated with microparticles capable of tailorable delivery of two different growth factors was engineered to regulate endochondral ossification. We used gelatin microparticles (GM) to deliver TGF-β1 to first induce cartilage formation and mineral-coated hydroxyapatite microparticles (MCMs) to deliver osteogenic [23] and chondrogenic [24] factor BMP-2 in a more sustained manner to facilitate cartilage remodeling into bone. BMP-2 can promote chondrocyte proliferation and hypertrophy [25], a key step in endochondral ossification. In fact, BMP-2 signaling has been shown to be essential for endochondral ossification [26–28] and to induce endochondral ossification in fracture repair [29]. Therefore, adding BMP-2 to this high-density system may prove valuable in recapitulating endochondral ossification. MCM was chosen to deliver BMP-2 because hydroxyapatite is both osteoinductive and osteoconductive and can serve as a mineral source. Importantly, the mineral coating of MCM has a high affinity for proteins, and therefore MCMs are capable of binding, sequestering, and delivering growth factors such as BMP-2 and VEGF in a tailorable manner [30] for bone tissue engineering. Incorporation of only BMP-2-releasing MCMs within hMSC aggregates has previously been used to engineer bone-like tissue [31].

In this work, soluble TGF-β1 and BMP-2 were first sequentially presented at various defined times in culture media to hMSC aggregates to determine when switching to BMP-2 treatment would best partially recapitulate endochondral ossification. The combination of GM and MCM for locally delivering TGF-β1 and BMP-2, respectively, in a spatiotemporally controlled manner within hMSC aggregates may allow for greater control over the process of endochondral bone formation compared with delivering BMP-2 alone. We hypothesized that early release of TGF-β1 from GM could catalyze the formation of a cartilage template for endochondral bone formation, and then prolonged BMP-2 delivery could promote the replacement of the cartilage anlage with vascularized bone. For clinical applications, this self-sustaining microparticle-incorporated system may be more readily implanted in vivo to treat critical-sized bone defects without the need for a vascular supply or repeated growth factor supplementation.

MATERIALS AND METHODS

hMSC Isolation and Expansion

hMSCs were isolated from the posterior iliac crest of 3 healthy male donors (43 $\pm$ 5 years) using a protocol approved by the University Hospitals of Cleveland Institutional Review Board and cultured as previously described [32]. Briefly, the aspirates were rinsed with low-glucose Dulbecco's modified Eagle's medium (DMEM; Sigma-Aldrich, St. Louis, MO, http://www.sigmaaldrich.com) with 10% prescreened fetal bovine serum (Gibco, Grand Island, NY, http://www.thermofisher.com). Mononucleated cells were isolated using a Percoll (Sigma-Aldrich) density gradient, plated on tissue

culture plastic at a density of 1.8×10^5 cells per cm^2 in medium containing 10 ng/ml fibroblast growth factor-2 (R&D Systems Inc., Minneapolis, MN, http://www.rndsystems.com), and cultured at 37°C with 5% CO_2. Nonadherent cells were removed after 4 days. The adherent cells, primary hMSCs, were cultured for another 10–14 days with medium changes every 3 days. They were then reseeded at 4×10^3 cells per cm^2 and expanded until passage 2, when they were stored in liquid nitrogen in fetal bovine serum with 10% dimethyl sulfoxide until use.

GM Synthesis and TGF-β1 Loading and Release

GM were synthesized using a water-in-oil single emulsion technique and cross-linked with genipin for 2 hours as previously described [19–21]. Briefly, 11.1% wt/vol acidic gelatin (Sigma-Aldrich) was dissolved in deionized water (diH_2O), added dropwise into 250 ml of preheated (45°C) olive oil (Gia Russa, Coitsville, OH, http://www.giarussa.com), and magnetically stirred at 500 rpm. After 10 minutes, stirring ensued at 4°C for 30 minutes. 100 ml of acetone chilled at 4°C was added to the emulsion and again an hour later. The stirring rate was increased to 1,000 rpm for 5 minutes, after which the solution was filtered, and the resulting emulsions were washed with acetone and dried overnight. GM were then cross-linked with 1% wt/vol genipin (Wako USA, Richmond, VA, http://www.wako-chem.co.jp/english) on a magnetic stir plate at room temperature (RT). After 2 hours, the cross-linked GM were rinsed with diH_2O and lyophilized.

To load TGF-β1, UV-sterilized GM were incubated in phosphate-buffered saline (PBS) containing TGF-β1 (400 ng/mg GM; Peprotech, Rocky Hill, NJ, http://www.peprotech.com) for 2 hours at 37°C as previously described [19–21]. To ensure 100% binding efficiency of TGF-β1 to the GM, the volume of TGF-β1 solution used was less than the equilibrium swelling volume of the GM. To analyze TGF-β1 release, 5 mg of GM was incubated in 0.5 ml of PBS solution of TGF-β1 and 0.2% ^{125}I-TGF-β1 at a loading concentration of 400 ng of TGF-β1/mg GM at 37°C ($n = 6$). After 2 hours, 0.5 ml of PBS containing 2 ng/ml collagenase (Sigma-Aldrich) was added, and samples were further incubated at 37°C. To determine the amount of TGF-β1 released at specific time points, the supernatant was collected and replaced with fresh collagenase-containing PBS (2 ng collagenase/ml), and the radioactivity in the supernatant was measured using a 1450 MicroBeta Trilux Liquid Scintillation and Luminescence Counter (PerkinElmer Life and Analytical Sciences, Waltham, MA, http://www.perkinelmer.com).

MCM Synthesis and BMP-2 Loading and Release

Hydroxyapatite (HA) microparticles ranging from 3 to 5 μm in diameter from Plasma Biotal LTD (Derbyshire, U.K., http://www.plasma-biotal.com) were mineral-coated in modified simulated body fluid (mSBF) and loaded with BMP-2 as previously described [30]. Briefly, HA microparticles were added at 2 mg/ml to mSBF (pH 6.8) containing 141 mM NaCl, 4.0 mM KCl, 0.5 mM $MgSO_4$, 1.0 mM $MgCl_2$, 20.0 mM HEPES, 5.0 mM $CaCl_2$, 2.0 mM KH_2PO_4, and 4.2 mM $NaHCO_3$. The solution was stirred continuously at 37°C for 7 days with the mSBF refreshed daily. At the end of the coating process, the MCMs were rinsed with diH_2O and lyophilized.

BMP-2 (Dr. Walter Sebald, Department of Developmental Biology, University of Würzburg, Germany, https://www.uni-wuerzburg.de/startseite/) was loaded at 6,400 ng/mg MCM by incubating UV-sterilized MCM in BMP-2-containing PBS at 37°C for 4 hours. The BMP-2-loaded MCMs were then centrifuged at 800 $\times$ g for 2 minutes, and the resulting MCMs were washed twice with PBS. A binding efficiency of 60% was taken into account during loading [30]. For conditions without BMP-2 loading, empty MCM were incubated with PBS only and treated similarly. BMP-2 release from MCM was analyzed as previously described [30]. Briefly, 1 mg of BMP-2 (0.5% ^{125}I-BMP-2) in 1 ml of PBS was loaded onto 5 mg of MCM. After centrifugation and two PBS washes, the BMP-2-loaded MCMs were incubated in PBS at 37°C. At specific time points, the amount of BMP-2 in the supernatant ($n = 6$) was determined by measuring the radioactivity in each solution with a Packard Cobra II γ Counter (PerkinElmer Life and Analytical Sciences).

Microparticle-Incorporated Aggregate Production and Culture

Microparticle-incorporated hMSC aggregates were formed in a similar manner as previously described [20]. Briefly, passage 3 hMSCs (2.5×10^5) were suspended in serum-free basal medium with or without TGF-β1-loaded GM (400 ng of TGF-β1 per mg GM; 0.15 mg of GM per aggregate) and/or MCM with or without BMP-2 (6,400 ng of BMP-2 per mg of MCM; 0.05 mg of MCM per aggregate). Two hundred microliter aliquots were centrifuged in a V-bottom polypropylene 96-well plate to form aggregates. Aggregates were cultured in either basal medium or chondrogenic medium for 2 weeks followed by osteogenic medium with or without 100 ng/ml BMP-2 for an additional 3 weeks. Basal medium consisted of high glucose DMEM (DMEM-HG) with 10% ITS$^+$ Premix, 100 nM dexamethasone, 37.5 μg/ml L-ascorbic acid-2-phosphate, 1 mM sodium pyruvate, 100 μM nonessential amino acids. Chondrogenic medium was defined as basal medium with exogenous (exo.) TGF-β1 (10 ng/ml). Osteogenic medium contained DMEM-HG with 10% ITS$^+$ Premix, 1 mM sodium pyruvate, 100 μM nonessential amino acids, 100 nM dexamethasone, 50 μg/ml L-ascorbic acid-2-phosphate, and 5 mM β-glycerophosphate. The total dose of TGF-β1 presented exogenously to the cells at the conventional media concentration of 10 ng/ml [18, 33] for the first 2 weeks of culture was 16 ng, and the amount of TGF-β1 loaded onto the GMs was 60 ng per aggregate. The specific conditions of GM incorporation, TGF-β1 loading concentration, and GM amount used in this study were based on previously published data [20] and chosen to ensure strong hMSC chondrogenesis for the formation of a successful cartilage template for endochondral ossification. The total dose of BMP-2 presented exogenously to the cells at the conventional media concentration of 100 ng/ml [34] for the last 3 weeks of culture was 240 ng, and the amount loaded onto the MCM was approximately 320 ng, assuming 60% binding efficiency [30]. Because all microparticle incorporation took place during aggregate production and hence at the beginning of the culture period, the higher BMP-2 amount used for loading onto the MCM was chosen to take into account the release of BMP-2 from the microparticles during the first 2 weeks of culture. Aggregates were cultured for 5 weeks with the medium changed every other day. After 2 and 5 weeks, aggregates ($n = 4$) were harvested and stored in −20°C until analysis.

Aggregate Sizing

Frozen aggregates ($n = 4$ per group; donor B) were thawed in PBS and imaged using an Olympus BX61VS microscope (Olympus, Center Valley, PA, http://www.olympusamerica.com) equipped

with a Pike F-505 camera (Allied Vision Technologies, Stadtroda, Germany, https://www.alliedvision.com). The diameter of each aggregate was obtained by averaging measurements at 3 different positions (12 to 6, 2 to 8, and 4 to 10 o'clock) using ImageJ software (NIH, Washington, DC, http://www.nih.gov).

Biochemical Analysis

Harvested aggregates ($n = 4$) were assayed for DNA, GAG, calcium content, and alkaline phosphatase (ALP) activity. Briefly, aggregates were homogenized for 1 minute in papain buffer. ALP lysis buffer (1 mM $MgCl_2$, 20 μm $ZnCl_2$, and 0.1% octyl-β-glucopyranoside in 10 mM Tris buffer at pH 7.4) was added to half of each sample. Using an ALP assay kit (Sigma-Aldrich) according to the manufacturer's instructions, ALP activity was determined by measuring the amount of 4-nitrophenol after a 30-minute incubation with p-nitrophenol phosphate at 37°C. The other half of each sample was subjected to overnight papain digestion at 65°C. The next day, a fraction of this half of the samples was assayed for calcium content using an o-cresophthalein complexone assay (Sigma-Aldrich) after receiving 1 M HCl treatment to dissolve MCM. The remainder of this half of the samples was treated with 10% EDTA in 0.05 M Tris-HCl buffer (pH 7.4) to dissociate DNA and/or protein from MCM. DNA content was then determined using Quant-iT PicoGreen dsDNA assay kit (Invitrogen, Carlsbad, CA, http://www.invitrogen.com), and GAG was measured with a dimethyl-methylene blue assay [35].

Histological Analysis

After 2 and 5 weeks of culture aggregates designated for histological examination ($n = 4$) were fixed overnight in 10% neutral buffered formalin and paraffin-embedded. Sections of 5 μm were stained for GAG via Safranin O (Saf O)/Fast Green and calcium with alizarin red S (ARS). Immunohistochemistry was performed to examine the presence of types I and II collagen (Col I and Col II), osteocalcin (OCN), and osteopontin (OPN). All sections were deparaffinized and rehydrated with decreasing concentrations of ethanol, and endogenous peroxidase activity was quenched by submerging the samples in 30% vol/vol hydrogen peroxide/methanol (1:9) for 10 minutes. For epitope retrieval, sections for Col I and Col II staining were digested with PBS containing Protease (1 mg/ml; Sigma-Aldrich) at RT for 15 minutes, whereas those designated for OCN and OPN staining were treated with citrate-based antigen retrieval buffer (Vector Laboratories, Burlingame, CA, http://www.vectorlabs.com) at 60°C for 20 minutes. Anti-Col I (ab34710; Abcam, Cambridge, MA, http://www.abcam.com), anti-Col II (ab34712; Abcam), anti-OPN (ab8448; Abcam), and anti-OCN (ab93876; Abcam) were used as primary antibodies, and rabbit IgG (Vector Laboratories) was used as a negative control. The Histostain-Plus Bulk kit (Invitrogen) was used with aminoethyl carbazole (Invitrogen) in accordance with the manufacturer's instructions. Slides were mounted with glycerol vinyl alcohol (Invitrogen) and imaged using an Olympus BX61VS microscope.

Quantitative analysis of ARS staining ($n = 5$–6 per group; 1 section per sample; all three donors) was performed using a slight modification of a previously published methodology [36]. First, black and white image masks of the ARS-stained color images were created using the wand tool (tolerance: 60) in Photoshop CS6 software (Adobe Systems, San Jose, CA, http://www.adobe.com) to highlight areas of calcification across the aggregates. ARS-stained areas were designated in black, whereas the remaining area was designated in white, creating specific masks for analysis. Using the magnetic lasso tool in Photoshop, the aggregates were outlined
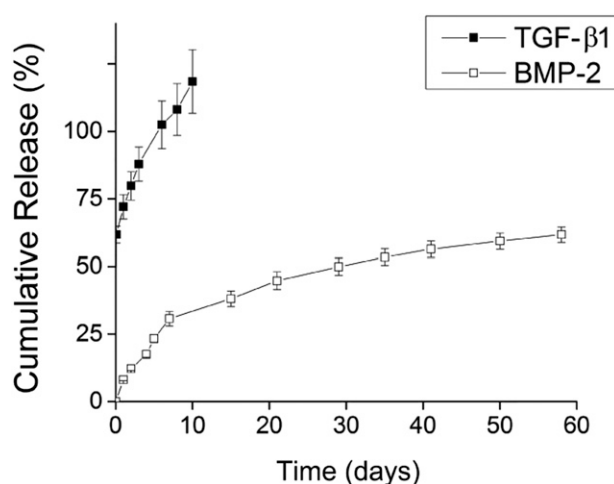

Figure 1. Cumulative release of TGF-β1 from gelatin microparticles in collagenase-containing phosphate-buffered saline (PBS; black) and BMP-2 from mineral-coated hydroxyapatite microparticles in PBS (white). Abbreviation: BMP, bone morphogenetic protein; TGF, transforming growth factor.

to create a mask (mask 1) for total area analysis. Next, the mask was reduced to 50% of its size while maintaining the aspect ratio, creating a mask representing the aggregate core (mask 2). To assess ARS staining within the aggregate core, the ARS-highlighted black and white image mask of the whole aggregate was overlaid with the semitransparent mask 2. To assess ARS staining within the periphery, the core area was subtracted from the total area to create mask 3 and the ARS-highlighted black and white image mask of the total area was overlaid with mask 3. Using the default wand tool in ImageJ software, the combined black-colored areas were calculated as ARS-stained area distinguishing between the aggregate core and periphery.

Statistical Analysis

Statistical analysis was performed using InStat 3.06 software (GraphPad Software Inc., La Jolla, CA, http://www.graphpad.com). One-way analysis of variance with Tukey's post hoc tests was used to compare between time points for each condition and between conditions at each time point. For the quantification of ARS staining, the same analysis was used to compare between regions (e.g., core versus periphery) for each condition and between conditions in each region. Differences were considered statistically significant at $p < .05$. All data are presented as the averages $\pm$ the standard deviation.

Microparticle Characterization and Growth Factor Release

GMs had an average diameter of 60.9 $\pm$ 50.1 μm and cross-linking density of 28.8 $\pm$ 6.8% [21]. Because collagenases secreted by cells in the aggregate will ultimately contribute to enzymatic degradation of GM and TGF-β1 release, GM were incubated in collagenase-containing PBS to determine the theoretical TGF-β1 release profile. Early release of loaded TGF-β1 from GM was achieved with an initial burst of ~60%, and all loaded TGF-β1 was released by day 10 (Fig. 1). In contrast, MCMs (average

diameter of 3.41 ± 1.04 μm) were capable of more sustained re-lease of its BMP-2 payload with no initial burst and only 60% of loaded BMP-2 released by day 60 (Fig. 1).

Morphological and Biochemical Analysis of Aggregates

Aggregates from three hMSC donors were sequentially cultured in chondrogenic media with TGF-β1 and then in osteogenic media containing BMP-2 to determine the time course that best pro-moted in vitro endochondral ossification (supplemental online Table 1). Sequential presentation of soluble growth factors resulted in varying degrees of chondrogenesis, ALP expression, and miner-alization that depended on the time course presented, demonstrat-ing the importance of the timing of sequential growth factor treatment in regulating endochondral ossification. The results showed that switching to BMP-2 treatment after 2 weeks of chon-drogenesis with TGF-β1 is most effective for regulating the replace-ment of cartilage with bone (supplemental online Figs. 1–5).

Following the chosen time course of 2 weeks of chondrogenic differentiation followed by 3 weeks of osteogenic treatment, ag-gregates were incorporated with microparticles capable of con-trolled, localized delivery of TGF-β1 and BMP-2 and cultured (Fig. 2). To evaluate the impact of the different culture conditions on aggregate size, the average diameters of week 5 aggregates from donor B were measured (Fig. 3A). At week 2 and 5, aggre-gates were analyzed for DNA, GAG/DNA, and calcium content and ALP activity for each donor, and the averages for each donor were pooled and averaged (Fig. 3B–3E). The data for each individ-ual donor are shown in supplemental online Figures 6 and 7.

Aggregate Size

Whole aggregates in groups 2 and 3 were significantly smaller than all other groups with the exception of group 2 compared with group 5 (Fig. 3A). These results corroborate histological data, which showed aggregate sections in groups 2 and 3 appearing smaller than the other groups.

Cell Content

After 2 weeks, DNA content was similar among groups 1–5 for all donors (Fig. 3B; supplemental online Fig. 6). Group 6, in which in-corporated GM and MCM were loaded with TGF-β1 and BMP-2, respectively, was significantly higher than cell-only group 1. By week 5, DNA content significantly decreased in each group with all groups exhibiting similar DNA levels.

GAG/DNA Content

At week 2, groups 2 and 3, which were only incorporated with MCM, were lower than group 1 (Fig. 3C). Groups 4 and 6, in which aggregates were incorporated with TGF-β1-loaded GM, had significantly higher GAG/DNA than groups 1–3. Al-though group 5 also had incorporated TGF-β1-loaded GM, it had lower GAG/DNA content compared with groups 4 and 6 at this early time point. By week 5, significant increases in GAG production were observed in each group. Groups 2 and 3 had the lowest average GAG/DNA contents, which were sig-nificantly lower than group 4.

ALP Activity

At week 2, ALP activity was highest in group 6 (Fig. 3D). Significant increases were observed in all groups by week 5. No statistical significance was found among the groups at this later time
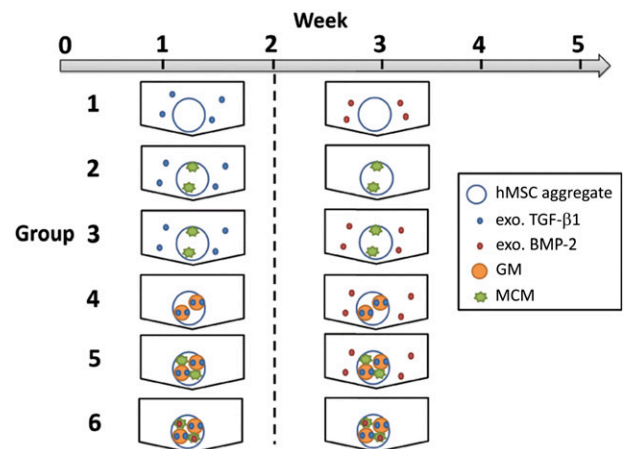

Figure 2. Experimental conditions for microparticle-incorporated hMSC aggregate study. Aggregates were cultured with chondrogenic signals for 2 weeks and then with osteogenic signals for 3 weeks. Abbreviations: BMP, bone morphogenetic protein; GM, gelatin microparticle; hMSC, hu-man bone marrow-derived mesenchymal stem cell; MCM, mineral-coated hydroxyapatite microparticle; TGF, transforming growth factor.

point. However, ALP activity was variable among the donors (supplemental online Fig. 7).

Calcium Content

At week 2, only the amount of calcium initially incorporated in MCM-treated aggregates (groups 2, 3, 5, and 6) was measured (Fig. 3E). By week 5, mineralization took place in each group for all donors as significant increases in calcium content were observed. Further, groups 2, 3, 5, and 6 had significantly higher calcium content than groups 1 and 4 at this time point. Similar trends were found for each individual donor at week 5 with groups 1 and 4 exhibiting signifi-cantly lower calcium content compared with all other groups, which had similar levels of calcium (supplemental online Fig. 7).

Histological Analysis of Microparticle-Incorporated hMSC Aggregates

Sections of week 2 and 5 aggregates were stained for GAG and calcium. Representative sections from donor B are shown in Figures 4–7. At week 2, GAG and calcium staining confirmed biochemical results (Fig. 4). Groups 1–3 stained less intensely and less uniformly for GAG compared with groups 4–6 (Fig. 4A). Although a fraction of partially degraded GM that stained blue in the Saf O/Fast Green histology still remained in group 4, all incorporated GM in groups 5 and 6 were completely de-graded by this early time point. As for calcium, positive staining was only observed in aggregates with incorporated MCM (groups 2, 3, 5, and 6) (Fig. 4B). Because calcium content at week 2 was similar to the amount of calcium initially incorpo-rated in MCM-treated aggregates (Fig. 3E), it is likely that most of the positive ARS staining was of the incorporated MCM.

By week 5, the aggregate core stained intensely for GAG, whereas the outer shell was positive for calcium in group 1 (Fig. 5A, 5C). Aggregates in groups 2 and 3 were smaller (Fig. 3A) and exhibited weaker GAG staining (Fig. 5A) than the other groups. Consistent with the biochemical data, group 4 stained most intensely for GAG, but calcium staining was only positive in small regions of the outer shell of the aggregates. On the other
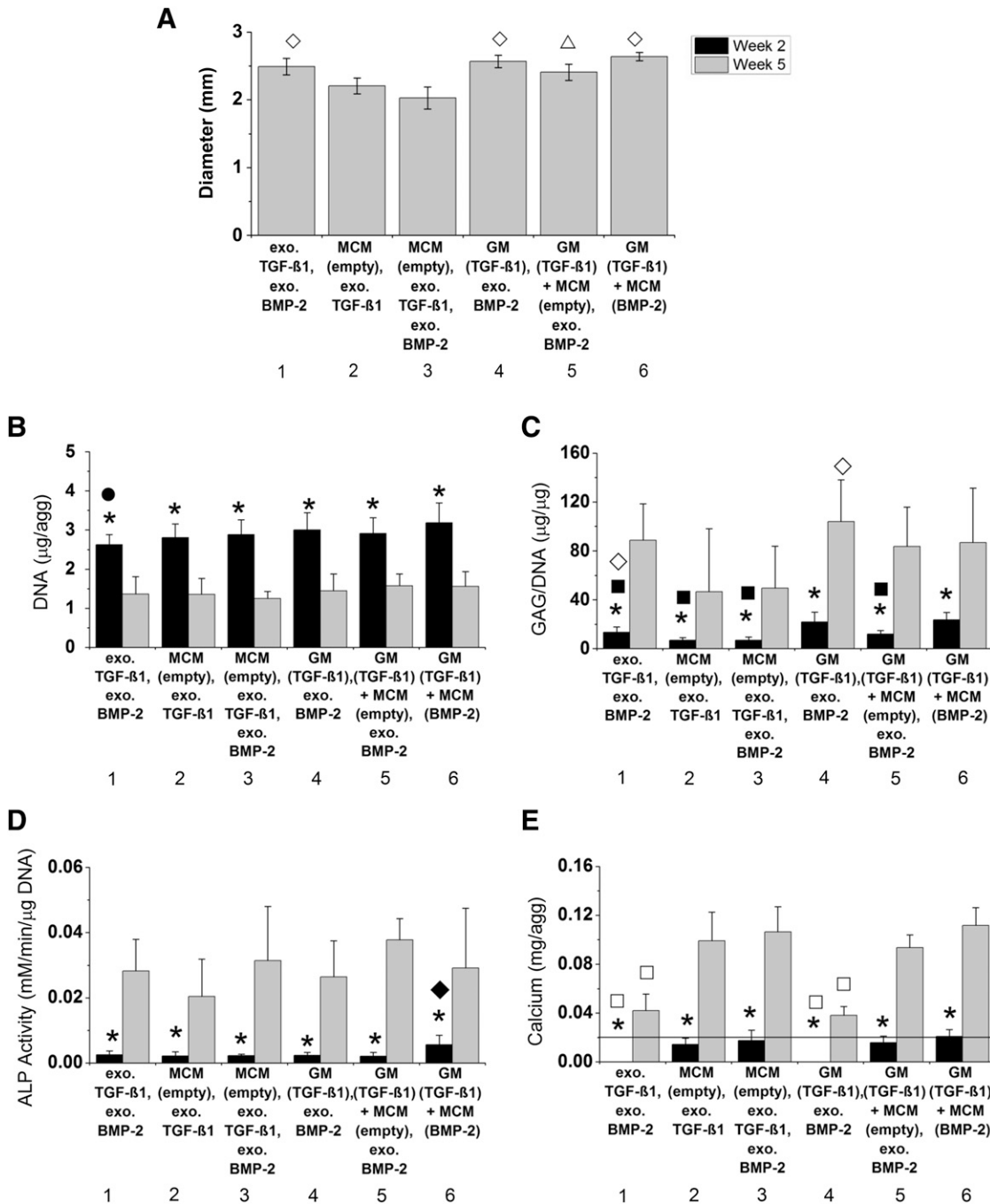
Figure 3. Diameter and biochemical content of microparticle-incorporated hMSC aggregates. **(A):** Diameters of whole aggregates from a representative donor (donor B) after 5 weeks of culture. **(B–E):** Average DNA content **(B)**, GAG/DNA content **(C)**, ALP activity **(D)**, and calcium content in weeks 2 (black) and 5 (gray) aggregates **(E)** for three different hMSC donors. The line in **(E)** denotes amount of calcium initially within each MCM-containing aggregate assuming 100% incorporation efficiency. ∗, significantly different between time points. ◊, significantly different from groups 2 and 3; △, significantly different from group 3; ●, significantly different from group 6; ■, significantly different from groups 4 and 6; ◆, significantly different from all other groups; ▢, significantly different from groups 2, 3, 5, and 6 at specific time point. Abbreviations: ALP, alkaline phosphatase; BMP, bone morphogenetic protein; exo., exogenous; GAG, glycosaminoglycan; GM, gelatin microparticle; MCM, mineral-coated hydroxyapatite microparticle; TGF, transforming growth factor.

hand, intense GAG staining in aggregates of groups 5 and 6 was mainly limited to areas that did not stain for calcium. In general, GAG and calcium staining corresponded to the biochemical results for all donors, with the weakest GAG staining in groups 2 and 3 and intense calcium staining in groups 2, 3, 5, and 6 at week 5.

Higher magnification images of GAG staining revealed the presence of cells with chondrocyte-like morphology in Saf O-stained regions in all groups with a greater presence of larger, round cells that are representative of hypertrophic chondrocytes in groups 5 and 6 compared with the other groups (Fig. 5B) [37].
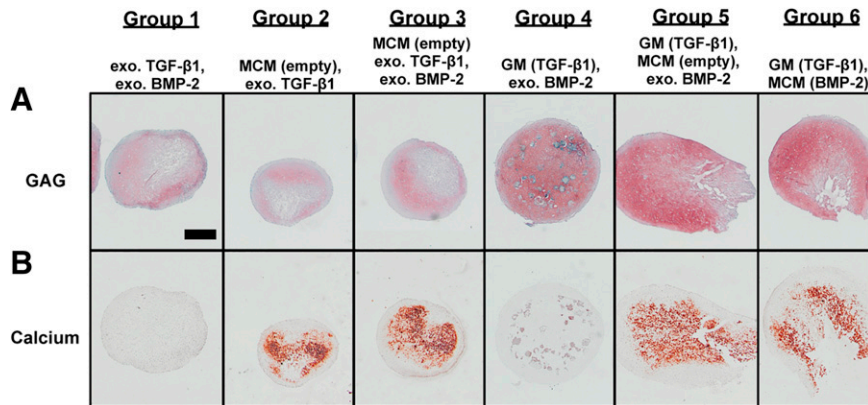
Figure 4. Photomicrographs of histology from a representative donor at week 2. **(A):** Photomicrograph of Safranin O/Fast Green histology of week 2 aggregates from donor B. **(B):** Photomicrograph of alizarin red S histology of week 2 aggregates from donor B. Round blue regions represent incorporated GM that had not completely degraded. Scale bars = 500 μm. All images are at the same scale. Abbreviations: BMP, bone morphogenetic protein; exo., exogenous; GAG, glycosaminoglycan; GM, gelatin microparticle; MCM, mineral-coated hydroxyapatite microparticle; TGF, transforming growth factor.

Corresponding higher magnification images of ARS staining showed colocalization of GAG staining with positive staining for mineralization, suggesting the presence of calcified hypertrophic cartilage in all groups (Fig. 5B, 5D). Additionally, the presence of calcium-stained regions that did not also stain for GAG was most prominent in group 6, providing evidence of mineralized bone tissue within aggregates in this group.

Quantitative analysis of calcium staining revealed more extensive staining in the periphery compared with the core of the aggregate in each group (Fig. 5E). In the core, the amount of ARS staining in groups 1 and 4 was significantly lower than all other groups. In the peripheral region, groups 1 and 4 also exhibited less staining compared with the other groups, but there was only statistical significance between groups 4 and 6.

Immunohistochemical staining of week 5 aggregates for Col I and II was performed to confirm the presence of neocartilage and bone-like tissue, respectively (Fig. 6). In group 1, staining for Col I and II occurred throughout the core of the aggregates. In the outer shell, Col I stained intensely, whereas no Col II staining was observed. Although intense Col I staining resulted in groups 2 and 3 with extensive staining throughout group 3 aggregates, weaker Col II staining limited to small regions resulted in group 2. Similar to group 1, group 4 exhibited staining for Col I and II throughout the aggregates with stronger staining for Col I than Col II in certain regions and vice versa in other regions. Similar to groups 2 and 3, Col I staining in group 5 was stronger and more extensive than Col II staining. In group 6, staining was localized to specific regions within the aggregates for the different types of collagen. Interestingly for this group, intense Col I staining corresponded to regions that also stained for calcium. Col II staining was observed in regions that also exhibited GAG staining. Regions that stained intensely for one collagen type had either light or negative staining for the other type.

In addition to collagen, week 5 aggregate sections were also immunostained for OPN and OCN to assess the amount and distribution of these late bone matrix markers (Fig. 7). Positive staining, although relatively weaker and less extensive than Col I staining, was observed in most groups for OCN (Fig. 7A) and in all groups for OPN (Fig. 7B). In general, staining for both markers was localized to the mineralized regions of the aggregates with generally more intense staining observed for OPN than OCN in each group. Similar to donor B, donors A and C exhibited GAG and calcium staining that supported their respective biochemical data and localized staining for cartilage and bone markers.

DISCUSSION

With the ultimate goal of treating critically sized defects, this study explored the capacity to drive endochondral ossification of hMSC aggregates via controlled temporal presentation of chondrogenic and osteogenic growth factors from within the cellular constructs for bone tissue engineering applications. In contrast to scaffold-based approaches, the high-density nature of cells in aggregates provides a biomimetic microenvironment with abundant cell-cell interactions that emulates the mesenchymal condensation process critical to both bone formation pathways. High-density cultures have also been extensively explored for chondrogenesis, a vital step in endochondral ossification. Further, the absence of a scaffold bypasses the need to synchronize scaffold degradation with new tissue formation, a challenging feat that could compromise the integrity of the engineered construct if not achieved.

Endochondral ossification has been recapitulated in both high-density cultures [11–15] and scaffold-based constructs [12, 38–41]. In these systems, cells were chondrogenically primed with a chondroinductive factor such as TGF-β1 for at least 3 weeks to produce mature cartilaginous anlages prior to implantation. In several systems, cells were also treated with hypertrophic factors and/or osteogenic factors after chondrogenic priming to ensure the formation of hypertrophic cartilage [12, 14, 15, 38]. Because BMP-2 is a major player in endochondral ossification [26, 27, 29] and its positive effects on this pathway were demonstrated recently in MCM-incorporated hMSC aggregates [31], the effects of BMP-2 treatment after chondrogenic priming with TGF-β1 in enhancing cartilage remodeling into bone was investigated. Compared with other factors used after chondrogenic priming, BMP-2 may be a better candidate for clinical translation because it is already used extensively in the clinical setting to repair bone [42, 43].
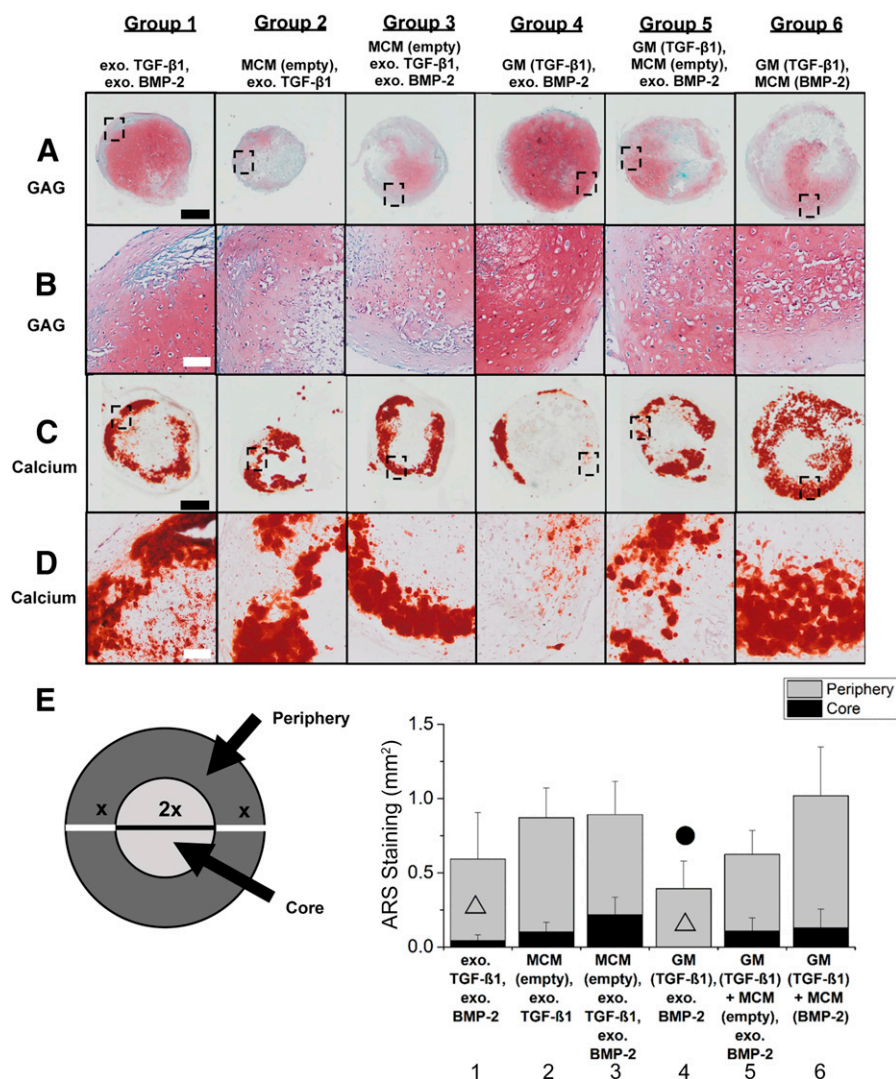
Figure 5. Photomicrographs of histology from a representative donor at week 5 and quantification of ARS staining for all 3 donors. **(A, C)**: Photomicrographs of Safranin O (Saf O)/Fast Green **(A)** and ARS **(C)** histology of week 5 aggregates from donor B. **(B, D)**: Higher magnification images of Saf O/Fast Green **(B)** and ARS **(D)** staining of same region in each group as indicated by black rectangles in **(A)** and **(C)**, respectively. Scale bars = 500 μm (black), 100 μm (white). All images in each row are at the same scale. **(E)**: Quantification of average ARS staining in the periphery and core of week 5 aggregates for all three donors. $\triangle$, significantly different from group 3; ●, significantly different from group 6. Abbreviations: ARS, alizarin red S; BMP, bone morphogenetic protein; exo., exogenous; GAG, glycosaminoglycan; GM, gelatin microparticle; MCM, mineral-coated hydroxyapatite microparticle; TGF, transforming growth factor.

A comparison study was first performed to determine how the sequential presentation of soluble TGF-β1 and BMP-2 in media to hMSC aggregates at various defined times influences the induction of endochondral ossification (supplemental online data). TGF-β1 was supplemented in serum-free chondrogenic medium, and BMP-2 was added to serum-free osteogenic medium. The defined time course of 2 weeks of TGF-β1 and 3 weeks of BMP-2 presentation that best promoted endochondral ossification was determined through biochemical and histological analyses.

A spatiotemporally controlled growth factor delivery system was then engineered for early release of TGF-β1 and more sustained release of BMP-2 that followed the aforementioned chosen time course. The tailorable delivery system consisted of genipin-cross-linked GM and MCM. In a release study performed in collagenase-containing PBS, all loaded TGF-β1 was released from GM within 10 days (Fig. 1). Additionally, a previous study

reported substantial degradation of GM of similar composition, size distribution, and degree of cross-linking incorporated within hMSC aggregates after 2 weeks, signifying that most of the loaded TGF-β1 was released by this time point [20]. BMP-2 release from MCM in PBS, on the other hand, was more sustained. Unlike TGF-β1, no initial burst was observed, and only ~60% of loaded BMP-2 was released over 60 days (Fig. 1). Therefore, GMs were expected to degrade quickly within hMSC aggregates via cell-mediated enzyme secretion providing early presentation of TGF-β1 to induce chondrogenesis, and MCMs within the aggregates would release BMP-2 in a more sustained manner to drive the later stages of endochondral ossification. Importantly, the cross-linking density of GM and the stability of the coating layer of MCM can be modified to tailor growth factor release, allowing for optimization of growth factor presentation to cells within the constructs [20, 44]. In contrast to previously reported systems, in which growth
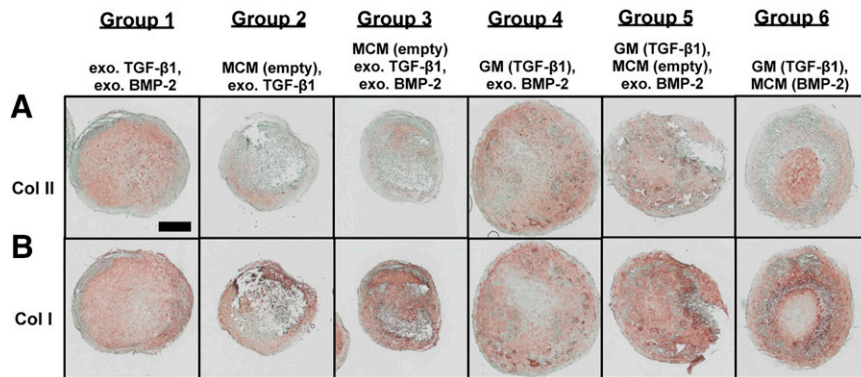
Figure 6. Photomicrographs of collagen immunohistochemical staining of week 5 aggregates from a representative donor. **(A):** Photomicrographs of Col II immunohistochemical staining of week 5 aggregates from donor B. **(B):** Photomicrographs of Col I immunohistochemical staining of week 5 aggregates from donor B. Scale bar = 500 μm. All images are at the same scale. Abbreviations: BMP, bone morphogenetic protein; Col, collagen; exo., exogenous; GM, gelatin microparticle; MCM, mineral-coated hydroxyapatite microparticle; TGF, transforming growth factor.
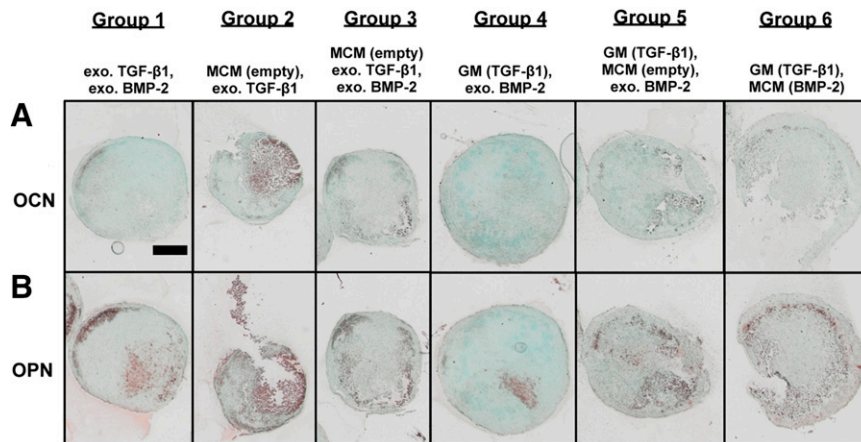

Figure 7. Photomicrographs of OCN and OPN immunohistochemical staining of week 5 aggregates from a representative donor. **(A):** Photomicrographs of OCN immunohistochemical staining of week 5 aggregates from donor B. **(B):** Photomicrographs of OPN immunohistochemical staining of week 5 aggregates from donor B. Scale bar = 500 μm. All images are at the same scale. Abbreviations: BMP, bone morphogenetic protein; exo., exogenous; GM, gelatin microparticle; MCM, mineral-coated hydroxyapatite microparticle; OCN, osteocalcin; OPN, osteopontin; TGF, transforming growth factor.

factors were supplemented in the media and spatial control of their presentation was limited, the microparticle-based delivery system provides controllable and localized growth factor delivery, potentially avoiding issues resulting from diffusion limitations. While exogenous presentation requires repeated supplementation that is neither time- nor cost-effective, incorporation of growth factor-loaded microparticles within cell constructs may allow for earlier construct implantation to repair defects without extended prior in vitro culture. The tailorability of this delivery system also enables control over the surrounding cellular microenvironment long after the construct is implanted.

Microparticle-incorporated aggregates were produced with hMSCs from three healthy donors and cultured in serum-free media following the chosen time course of growth factor presentation. More specifically, aggregates were cultured in basal media with or without exogenous TGF-β1 for 2 weeks followed by 3 weeks in osteogenic media with or without exogenous BMP-2. Because serum contains a rich variety of proteins that can affect cell behavior and varies in composition from batch to batch, the use of defined serum-free media in this study allowed for the roles of

these particular bioactive factors (i.e., TGF-β1 and BMP-2) on endochondral ossification to be more clearly defined.

After 2 weeks of culture, each group in all three donors had more than 2 μg of DNA per aggregate, the theoretical amount present in the total number of cells used to form each aggregate (assuming ~8 pg of DNA per nucleus [45]) (Fig. 3B; supplemental online Fig. 6). This suggests that some cell proliferation occurred by week 2. However, DNA content decreased by week 5 in all groups. This decreased cellularity may be a result of culturing with predominantly osteogenic factors after week 2. In a recent study, we observed that DNA content in hMSC aggregates cultured in osteogenic medium for 2 weeks was significantly less than the theoretical amount of DNA given the number of cells originally used to form each aggregate assuming 100% incorporation efficiency, and DNA content and aggregate size continued to decrease with increasing culture time [31]. Similarly, Burns et al. [46] reported shrinkage of aggregates after 21 days of culture in osteogenic medium. The decrease in DNA level may also be indicative of the occurrence of endochondral ossification during which the calcification of cartilage matrix leads to death of

hypertrophic chondrocytes. Thus, it may be that the lower DNA content resulted from the aggregates reaching that stage in the process.

When degree of chondrogenesis was assessed, aggregates incorporated with TGF-β1-loaded GM, with the exception of group 5, had significantly higher GAG/DNA content at week 2 than those receiving exogenous TGF-β1 treatment (groups 1–3) (Fig. 3C), signifying the importance of spatial distribution of TGF-β1 on chondrogenesis. Comparing the GM-incorporated groups (groups 4–6), the presence of MCM may have moderated GAG production (group 5), but this reduction was rescued by the earlier presentation of BMP-2 from incorporated MCM (group 6). This finding corroborates the reported role BMP-2 plays in chondrogenic differentiation of hMSCs in high-density cultures [24, 47, 48] and may explain why GAG production significantly increased in BMP-2-treated groups (groups 1 and 3–6) after week 2 despite the switch to osteogenic media. Additionally, aggregates treated with only MCM and exo. growth factor(s) (groups 2 and 3) had in general the lowest GAG/DNA content at week 5. Although only group 4 was significantly higher than groups 2 and 3 at this time point for the pooled data, cell-only aggregates (group 1) and aggregates incorporated with TGF-β1-loaded GM (groups 4–6) exhibited higher GAG production than groups 2 and 3 for each donor individually with the exception of group 2 for donor A, which was only significantly lower than groups 4 and 6 (supplemental online Fig. 6). These results suggest that the presence of MCM may be implicated in subduing chondrogenesis. Although groups 1 and 3 were cultured in the same media conditions, group 3 aggregates produced significantly less GAG than group 1, providing more evidence for the role of MCM in moderating GAG production in this system.

Because ALP is an early bone marker and is expressed by hypertrophic chondrocytes, ALP activity was also determined. At week 2, group 6 had the highest expression (Fig. 3D), suggesting that the BMP-2 delivered from the incorporated MCM may have enhanced ALP activity induced by TGF-β1. The increase in ALP expression in all groups by week 5 may be indicative of hypertrophic chondrocytes and/or osteoblasts residing within the constructs.

By week 5, ALP activity intensified in all groups with no statistical significance found between the groups (Fig. 3D). Interestingly, ALP activity at this time point was variable among the donors as shown by ALP content for each donor individually (supplemental online Fig. 7). Although expression was similar among all groups for donor C, groups 1 and 5 had significantly higher expression than all other groups except group 4 for donor A, and aggregates treated with both MCM and exo. BMP-2 (groups 3 and 5) exhibited the highest activity for donor B (supplemental online Fig. 7). These differences may be attributed to donor-to-donor variability. Cells from different donors may respond differently to specific signals. The significant difference between groups 2 and 3 for donor B may have resulted because cells from this donor may have been more responsive to exo. BMP-2 than cells from other donors. Furthermore, cells can respond at different rates. During osteogenesis, ALP activity peaks and then gradually decreases over time [49]. For donors A and B, local delivery of both TGF-β1 and BMP-2 from GM and MCM, respectively, may have promoted ALP activity in group 6 to peak earlier than week 5. This may, therefore, explain why expression in group 6 decreased to a level similar to (donor B) or lower than (donor A) in group 1 by week 5.

Donor response to mineralization, in contrast, was much more consistent (supplemental online Fig. 7). For all three donors, mineralization was observed in each group at week 5, with groups treated with both MCM and BMP-2 (groups 3, 5, and 6) having significantly higher calcium content than groups 1 and 4, indicating that the addition of MCM dramatically enhanced mineralization. This finding was corroborated in Dang et al. [31]. Although group 2 did not receive exo. BMP-2 treatment, its calcium content was similar to group 3, suggesting that MCM alone promoted mineralization. This is not surprising because hydroxyapatite has successfully been used as an osteoinductive mineral source [31, 50, 51]. These trends were confirmed when the calcium content data were pooled and averaged among the donors (Fig. 3E).

In general, histological staining verified the biochemical data and further supported the occurrence of endochondral ossification. Chondrogenesis was confirmed via positive staining for GAG and Col II in each group, with Col II staining localized to regions that also stained for GAG (Figs. 5A, 5B, 6A). Additionally, the localized staining observed for calcium, Col I, OPN, and OCN confirmed the existence of mineralized bone tissue (Figs. 5C, 5D, 6B, 7). In each group, regions that stained for both Col I and II were also observed, suggesting that cells in close proximity within the aggregates may respond differently to signals presented in their microenvironment (Fig. 6).

The heterogeneities observed in the histology suggest a spatial preference of osteogenesis at the periphery of the aggregates, whereas chondrogenesis occurred more in the aggregate core by week 5 (Fig. 5A, 5C, 5E). At week 2, Safranin O staining revealed generally more uniform GAG distribution throughout the aggregates in each group, whereas calcium staining was only observed in groups with incorporated MCM (Fig. 4). This was expected because all aggregates were exposed mostly to chondrogenic signals by this time point. As time progressed, osteogenic differentiation became more prominent. Because bone cells require more oxygen and nutrients than chondrocytes [5, 6], it is possible that cells on the periphery were more osteogenic because of the higher oxygen tension [52]. This may explain why calcium staining was more robust at the periphery at week 5 (Fig. 5E). Further, the decreased GAG staining at the periphery between weeks 2 and 5 suggests that some of the cartilage present earlier may have been replaced by bone via endochondral ossification (Figs. 4A, 5A).

Taken together, most mineralization occurred after cartilage formation as demonstrated by GAG production with minimal mineralization as early as week 2, indicating that endochondral ossification may have taken place by week 5. Immunohistochemistry also revealed the presence of cartilage and bone matrix markers further validating bone formation via a cartilaginous intermediate. Although groups 2 and 3 also exhibited high calcium levels at week 5, they exhibited the lowest GAG/DNA production (Fig. 3C, 3E), which may result in less cartilage remodeling into bone over time. Additionally, aggregates in groups 2 and 3 were significantly smaller with weaker staining for GAG and Col II compared with those in group 6 (Figs. 3A, 5–7). This suggests that incorporation of both growth factor-releasing GMs and MCMs may yield larger, more superior cartilage template for endochondral ossification. Although direct comparisons cannot be made because of the different systems and culture conditions, constructs with both GM and MCM in this study appear larger with higher DNA and GAG/DNA content than previously reported aggregates incorporated with only BMP-2-loaded MCM and without TGF-β1 treatment for the same three donors [31], motivating the use

of TGF-β1, and more specifically gelatin microparticles to deliver it, in this system. Furthermore, ALP activity and mineralization, in addition to GAG content, were observed at week 2 in MCM-incorporated aggregates treated with only BMP-2 for 2 of the 3 donors [31]. This suggests that BMP-2 induced not only chondrogenesis but also osteogenesis by this early time point. Thus, it is possible that some cells may have directly differentiated into osteoblasts via intramembranous ossification.

CONCLUSION

This study is the first to report a system of hMSC aggregates incorporated with bioactive microparticles capable of controlled spatiotemporal delivery of TGF-β1 and BMP-2 for bone tissue engineering via endochondral ossification. Compared with cell-only aggregates treated with exogenous growth factors at the conventional concentrations of TGF-β1 and BMP-2 (group 1), localized delivery of both TGF-β1 and BMP-2 from incorporated microparticles (group 6) resulted in enhanced endochondral bone formation. Specifically, chondrogenesis and osteogenesis were accelerated as demonstrated by GAG production and ALP activity, respectively, at week 2. Further, stronger mineralization and expression of bone matrix markers as shown by calcium production and immunohistochemical staining for Col I, OPN, and OCN, respectively, after 5 weeks were observed in group 6 aggregates subjected to local microparticle-mediated delivery of both factors than in group 1 aggregates. Notably, these results were achieved without requiring repeated growth factor dosing exogenously in the culture media. This work lays the foundation for a rapidly implantable tissue engineering system that promotes bone repair via endochondral ossification, a pathway that can delay the need for a functional vascular network and has an intrinsic ability to promote angiogenesis. The local delivery system may enable earlier implantation of the aggregates as the need for prior in vitro culture to prime the aggregates

with exogenously presented growth factors would not be necessary. The microparticles can deliver the growth factors in a tunable manner within the aggregates and potentially to the surrounding in vivo microenvironment long after the construct is implanted. Further, the modular nature of this system lends well to using different cell types and/or growth factors to induce endochondral bone formation, as well as production of other tissue types.

AUTHOR CONTRIBUTIONS

P.N.D.: conception and design, collection and assembly of data, data analysis and interpretation, manuscript writing, final approval of manuscript; N.D., L.M.P., and C.B.: collection and assembly of data; X.Y.: conception and design, collection and assembly of data, data analysis and interpretation; S.H. and L.D.S.: data analysis and interpretation; W.L.M.: conception and design, data analysis and interpretation; E.A.: conception and design, data analysis and interpretation, manuscript writing, final approval of manuscript.

DISCLOSURE OF POTENTIAL CONFLICTS OF INTEREST

W.L.M. is cofounder and director of Tissue Regeneration Systems Inc. and cofounder and director of Stem Pharm Inc. The other authors indicated no potential conflicts of interest.

REFERENCES

1 Jimi E, Hirata S, Osawa K et al. The current and future therapies of bone regeneration to repair bone defects. Int J Dent 2012;2012: 148261.

2 Habal MB, Reddi AH. Bone grafts and bone induction substitutes. Clin Plast Surg 1994;21: 525–542.

3 Meijer GJ, de Bruijn JD, Koole R et al. Cell-based bone tissue engineering. PLoS Med 2007; 4:e9.

4 Ishaug-Riley SL, Crane GM, Gurlek A et al. Ectopic bone formation by marrow stromal osteoblast transplantation using poly(DL-lactic-co-glycolic acid) foams implanted into the rat mesentery. J Biomed Mater Res 1997; 36:1–8.

5 Ishaug SL, Crane GM, Miller MJ et al. Bone formation by three-dimensional stromal osteoblast culture in biodegradable polymer scaffolds. J Biomed Mater Res 1997;36:17–28.

6 Coyle CH, Izzo NJ, Chu CR. Sustained hypoxia enhances chondrocyte matrix synthesis. J Orthop Res 2009;27:793–799.

7 Schipani E. Hypoxia and HIF-1alpha in chondrogenesis. Ann N Y Acad Sci 2006;1068: 66–73.

8 Petersen W, Tsokos M, Pufe T. Expression of VEGF121 and VEGF165 in hypertrophic chondrocytes of the human growth plate

and epiphyseal cartilage. J Anat 2002;201: 153–157.

9 Gerber HP, Vu TH, Ryan AM et al. VEGF couples hypertrophic cartilage remodeling, ossification and angiogenesis during endochondral bone formation. Nat Med 1999;5: 623–628.

10 Beamer B, Hettrich C, Lane J. Vascular endothelial growth factor: An essential component of angiogenesis and fracture healing. HSS J 2010;6:85–94.

11 Farrell E, van der Jagt OP, Koevoet W et al. Chondrogenic priming of human bone marrow stromal cells: A better route to bone repair? Tissue Eng Part C Methods 2009;15:285–295.

12 Farrell E, Both SK, Odörfer KI et al. In-vivo generation of bone via endochondral ossification by in-vitro chondrogenic priming of adult human and rat mesenchymal stem cells. BMC Musculoskelet Disord 2011;12:31.

13 Mueller MB, Tuan RS. Functional characterization of hypertrophy in chondrogenesis of human mesenchymal stem cells. Arthritis Rheum 2008;58:1377–1388.

14 Muraglia A, Corsi A, Riminucci M et al. Formation of a chondro-osseous rudiment in micromass cultures of human bone-marrow stromal cells. J Cell Sci 2003;116:2949–2955.

15 Scotti C, Tonnarelli B, Papadimitropoulos A et al. Recapitulation of endochondral

bone formation using human adult mesenchymal stem cells as a paradigm for developmental engineering. Proc Natl Acad Sci USA 2010;107: 7251–7256.

16 Steinert AF, Rackwitz L, Gilbert F et al. Concise review: The clinical application of mesenchymal stem cells for musculoskeletal regeneration: Current status and perspectives. STEM CELLS TRANSLATIONAL MEDICINE 2012;1:237–247.

17 Fell HB. The histogenesis of cartilage and bone in the long bones of the embryonic fowl. J Morphol 1925;40:417–459.

18 Johnstone B, Hering TM, Caplan AI et al. In vitro chondrogenesis of bone marrow-derived mesenchymal progenitor cells. Exp Cell Res 1998;238:265–272.

19 Solorio LD, Vieregge EL, Dhami CD et al. Engineered cartilage via self-assembled hMSC sheets with incorporated biodegradable gelatin microspheres releasing transforming growth factor-beta1. J Control Release 2012;158:224–232.

20 Solorio LD, Dhami CD, Dang PN et al. Spatiotemporal regulation of chondrogenic differentiation with controlled delivery of transforming growth factor-β1 from gelatin microspheres in mesenchymal stem cell aggregates. STEM CELLS TRANSLATIONAL MEDICINE 2012; 1:632–639.

21 Dang PN, Solorio LD, Alsberg E. Driving cartilage formation in high-density human adipose-derived stem cell aggregate and sheet

constructs without exogenous growth factor delivery. Tissue Eng Part A 2014;20:3163–3175.

22 Solorio LD, Fu AS, Hernández-Irizarry R et al. Chondrogenic differentiation of human mesenchymal stem cell aggregates via controlled release of TGF-beta1 from incorporated polymer microspheres. J Biomed Mater Res A 2010;92:1139–1144.

23 Luu HH, Song WX, Luo X et al. Distinct roles of bone morphogenetic proteins in osteogenic differentiation of mesenchymal stem cells. J Orthop Res 2007;25:665–677.

24 Schmitt B, Ringe J, Haupl T et al. BMP2 initiates chondrogenic lineage development of adult human mesenchymal stem cells in high-density culture. Differentiation 2003;71:567–577.

25 Leboy PS, Sullivan TA, Nooreyazdan M et al. Rapid chondrocyte maturation by serum-free culture with BMP-2 and ascorbic acid. J Cell Biochem 1997;66:394–403.

26 Tsumaki N, Yoshikawa H. The role of bone morphogenetic proteins in endochondral bone formation. Cytokine Growth Factor Rev 2005;16:279–285.

27 Rosen V. BMP2 signaling in bone development and repair. Cytokine Growth Factor Rev 2009;20:475–480.

28 Retting KN, Song B, Yoon BS et al. BMP canonical Smad signaling through Smad1 and Smad5 is required for endochondral bone formation. Development 2009;136:1093–1104.

29 Yu YY, Lieu S, Lu C et al. Bone morphogenetic protein 2 stimulates endochondral ossification by regulating periosteal cell fate during bone repair. Bone 2010;47:65–73.

30 Yu X, Khalil A, Dang PN et al. Multilayered inorganic microparticles for tunable dual growth factor delivery. Adv Funct Mater 2014;24:3082–3093.

31 Dang PN, Dwivedi N, Yu X et al. Guiding chondrogenesis and osteogenesis with mineral-coated hydroxyapatite and BMP-2 incorporated within high-density hMSC aggregates for bone regeneration. ACS Biomater Sci Eng 2015 (in press).

32 Haynesworth SE, Goshima J, Goldberg VM et al. Characterization of cells with osteogenic potential from human marrow. Bone 1992;13:81–88.

33 Solchaga LA, Penick KJ, Welter JF. Chondrogenic differentiation of bone marrow-derived mesenchymal stem cells: Tips and tricks. Methods Mol Biol 2011;698:253–278.

34 Honda Y, Ding X, Mussano F et al. Guiding the osteogenic fate of mouse and human mesenchymal stem cells through feedback system control. Sci Rep 2013;3:3420.

35 Farndale RW, Buttle DJ, Barrett AJ. Improved quantitation and discrimination of sulphated glycosaminoglycans by use of dimethylmethylene blue. Biochim Biophys Acta 1986;883:173–177.

36 Egan KP, Brennan TA, Pignolo RJ. Bone histomorphometry using free and commonly available software. Histopathology 2012;61:1168–1173.

37 Hunziker EB. Mechanism of longitudinal bone growth and its regulation by growth plate chondrocytes. Microsc Res Tech 1994;28:505–519.

38 Scotti C, Piccinini E, Takizawa H et al. Engineering of a functional bone organ through endochondral ossification. Proc Natl Acad Sci USA 2013;110:3997–4002.

39 Sheehy EJ, Vinardell T, Buckley CT et al. Engineering osteochondral constructs through spatial regulation of endochondral ossification. Acta Biomater 2013;9:5484–5492.

40 Liu K, Zhou GD, Liu W et al. The dependence of in vivo stable ectopic chondrogenesis by human mesenchymal stem cells on chondrogenic differentiation in vitro. Biomaterials 2008;29:2183–2192.

41 Yang W, Yang F, Wang Y et al. In vivo bone generation via the endochondral pathway on three-dimensional electrospun fibers. Acta Biomater 2013;9:4505–4512.

42 Ghodadra N, Singh K. Recombinant human bone morphogenetic protein-2 in the treatment of bone fractures. Biologics 2008;2:345–354.

43 Carreira AC, Alves GG, Zambuzzi WF et al. Bone morphogenetic proteins: Structure, biological function and therapeutic applications. Arch Biochem Biophys 2014;561:64–73.

44 Kimura M, Toyoda M, Gojo S et al. Allogeneic amniotic membrane-derived mesenchymal stromal cell transplantation in a porcine model of chronic myocardial ischemia. J Stem Cells Regen Med 2012;8:171–180.

45 Kim YJ, Sah RL, Doong JY et al. Fluorometric assay of DNA in cartilage explants using Hoechst 33258. Anal Biochem 1988;174:168–176.

46 Burns JS, Rasmussen PL, Larsen KH et al. Parameters in three-dimensional osteospheroids of telomerized human mesenchymal (stromal) stem cells grown on osteoconductive scaffolds that predict in vivo bone-forming potential. Tissue Eng Part A 2010;16:2331–2342.

47 Sekiya I, Larson BL, Vuoristo JT et al. Comparison of effect of BMP-2, -4, and -6 on in vitro cartilage formation of human adult stem cells from bone marrow stroma. Cell Tissue Res 2005;320:269–276.

48 Noël D, Caton D, Roche S et al. Cell specific differences between human adipose-derived and mesenchymal-stromal cells despite similar differentiation potentials. Exp Cell Res 2008;314:1575–1584.

49 Jaiswal N, Haynesworth SE, Caplan AI et al. Osteogenic differentiation of purified, culture-expanded human mesenchymal stem cells in vitro. J Cell Biochem 1997;64:295–312.

50 He P, Sahoo S, Ng KS et al. Enhanced osteoinductivity and osteoconductivity through hydroxyapatite coating of silk-based tissue-engineered ligament scaffold. J Biomed Mater Res A 2013;101:555–566.

51 Zhou H, Lee J. Nanoscale hydroxyapatite particles for bone tissue engineering. Acta Biomater 2011;7:2769–2781.

52 Holzwarth C, Vaegler M, Gieseke F et al. Low physiologic oxygen tensions reduce proliferation and differentiation of human multipotent mesenchymal stromal cells. BMC Cell Biol 2010;11:11.

See www.StemCellsTM.com for supporting information available online.